HOKKAIDO UNIVERSITY

Title	Remarkable enhancement of Cu catalyst activity in hydrogenation of dimethyl oxalate to ethylene glycol using gold
Author(s)	Wang, Ya-nan; Duan, Xinping; Zheng, Jianwei et al.
Citation	Catalysis Science & Technology, 2(8), 1637-1639 https://doi.org/10.1039/c2cy20154b
Issue Date	2012-08
Doc URL	https://hdl.handle.net/2115/52662
Rights	Catal. Sci. Technol., 2012,2, 1637-1639 - Reproduced by permission of The Royal Society of Chemistry (RSC)
Type	journal article
File Information	CST2-8_1637-1639.pdf

Hokkaido University Collection of Scholarly and Academic Papers : HUSCAP

Journal Name

Dynamic Article Links ►

Cite this: DOI: 10.1039/c0xx00000x

www.rsc.org/xxxxxx

ARTICLE TYPE

Remarkable enhancement of Cu catalyst activity in hydrogenation of dimethyl oxalate to ethylene glycol by using gold

Ya-nan Wang,[a] Xinping Duan,[a] Jianwei Zheng,[a] Haiqiang Lin,[a] Youzhu Yuan,* [a] Hiroko Ariga,[b] Satoru Takakusagi,[b] Kiyotaka Asakura* [b]

Received (in XXX, XXX) Xth XXXXXXXXX 20XX, Accepted Xth XXXXXXXXX 20XX

DOI: 10.1039/b000000x

The performance of an SBA-15 supported Cu catalyst for hydrogenation of dimethyl oxalate to ethylene glycol is markedly promoted with Au. A key genesis of the high activity of the catalyst is ascribed to the formation of Cu-Au alloy nanoparticles which stabilize the active species and retard their agglomeration during the hydrogenation process.

The indirect synthesis of ethylene glycol (EG) from coal is a potentially promising process, which involves the gasification of coal to syngas, followed by the coupling of CO with nitrite esters to oxalates and then the hydrogenation of oxalates to EG.[1,2] Copper-based catalysts have been discovered to be one of the most active materials for the vapor phase hydrogenation of dimethyl oxalate (DMO) to EG, but they has inherent problems of poor stability and short lifetime.[3-5] Finding a practical way to retain the state of highly dispersed copper has been proposed to be an important strategy to improve catalytic performance. Moreover, several recent works reveal that an appropriate Cu^0 and Cu^+ distribution is presumed to be a key in gaining excellent catalytic activity,[2,6,7] but more distinct evidences are highly demanded to be accumulated.

On the other hand, bimetallic catalysts have generated immense interest, since they offer a way to fine-tune the catalytic properties of metals.[8,9] Bimetallic Cu-Au systems are widely known to exhibit improved activity and selectivity in number of selective catalytic reactions including low-temperature CO oxidation,[10,11] selective alcohol oxidation,[12,13] selective hydrogenation.[14,15] However, the assignment of the active species of Cu-Au catalysts for some reactions is still ambiguous and controversial.[16,17]

Herein, we report that an SBA-15 supported Cu-Au bimetallic catalyst with Cu loading of 6 wt% and proper amount of Au prepared by two-step adsorption-$NaBH_4$ reduction process (see Experimental details in ESI) exhibit remarkable activity and thermal stability for the hydrogenation of DMO to EG. The structure-performance relationship of the catalyst is then addrssed by means of kinetic and spectroscopic studies.

The physicochemical properties of the catalysts characterized by powder X-ray diffraction (XRD), transmission electron microscopy (TEM) and nitrogen sorption are listed in Table 1s. The results indicated the successful synthesis of the $CuAu_x$/SBA-15 catalysts (Fig. 1s-3s). The vapor-phase DMO hydrogenation is comprised of DMO hydrogenation to methyl glycolate (MG), MG hydrogenation to EG and excessive hydrogenation to ethanol. Furthermore, there were byproducts of 1,2-propanediol (1,2-PDO) and 1,2-butanediol (1,2-BDO).[7,18] As shown in Table 1, the Cu/SBA-15 catalyst with copper loading of 6 wt% gave a DMO conversion of 71.5% and 38.2% selectivity to EG, while the 6 wt% Au/SBA-15 catalyst exhibited a much lower DMO conversion of 5.4% and about 80% selectivity to MG under the conditions of 453 K, 3.0 MPa, H_2/DMO molar ratio of 80 and weight liquid hourly space velocity ($WLHSV_{DMO}$) of 0.6 h^{-1}. When gold was introduced to Cu/SBA-15, the generated $CuAu_x$/SBA-15 catalysts (x stands for the atomic ratio of Au/Cu) were much more active than Cu/SBA-15 and Au/SBA-15 under similar reaction conditions. Their hydrogenation performance passed through a volcano type improvement as a function of Au content. The catalyst with a nominal atomic ratio of Au/Cu at 0.1 (actual ratio at 0.08) gave the highest performance of 100% conversion and 99.1% selectivity to EG. The enhancement became less apparent when the content of Au was further increased. When the $CuAu_{0.1}$/SBA-15 catalyst with a total metal loading of 6 wt% was employed, it produced a 100% conversion of DMO and 97.6% selectivity to EG. The results indicated that the Cu/Au atomic ratio has a significant effect on the catalytic behavoir of the $CuAu_x$/SBA-15 catalyst.

The excellent catalytic performance of $CuAu_{0.1}$/SBA-15 catalyst at 453 K was highly stable for over 240 h (Fig. 4s in ESI). In contrast, the Cu/SBA-15 catalyst showed a deactivation within 30 h even if the Cu loading was increased to 10 wt%, essentially owing to the obvious aggregation and coagulation of Cu nanoparticles (NPs) during the hydrogenation process (Fig. 5s in ESI). The stability of $CuAu_{0.1}$/SBA-15 catalyst was further evidenced by the catalytic performance after a heat treatment at 623 K for 24 h. The change of EG yield over the $CuAu_{0.1}$/SBA-15 catalyst before and after heat treatment was insignificant (Table 2s in ESI). In the case of $WLHSV_{DMO}$ at 0.6 h^{-1}, the selectivity to EG over the $CuAu_{0.1}$/SBA-15 catalyst was higher than 98% at temperatures ranging from 453 to 493 K (Fig. 6s in ESI). When the temperature was higher than 493 K, there was a main byproduct of EtOH due to the excessive hydrogenation of EG.[18] Furthermore, when the reaction temperature was set at 473 K, the

$CuAu_{0.1}$/SBA-15 catalyst could afford both DMO conversion and EG selectivity as high as 98% under a wide range of $WLHSV_{DMO}$ from 0.3 to 3.0 h^{-1} (Fig. 7s ESI), where the highest EG yield was exceptionally larger than 1500 mg/g-cat/h.

Table 1 Catalytic performance of $CuAu_x$/SBA-15 catalyst with different Au/Cu atomic ratio for hydrogenation of DMO

Catalyst	Conversion / %	Selectivity / %				TOF[a] / h^{-1}
		EG	MG	EtOH	Others[b]	
Cu/SBA-15	71.5	38.2	61.8	0	0	22
$CuAu_{0.05}$/SBA-15	84.7	41.8	58.2	0	0	37
$CuAu_{0.075}$/SBA-15	96.6	93.1	3.5	0.4	3.0	73
$CuAu_{0.1}$/SBA-15	100	99.1	0	0.8	0.1	121
$CuAu_{0.2}$/SBA-15	100	98.8	1.2	0	0.1	47
Au/SBA-15[c]	5.4	19.7	80.3	0	0	12
$CuAu_{0.1}$/SBA-15[d]	100	97.6	2.2	0	0.2	83

Reaction conditions: T=453 K, $WLHSV_{DMO}$=0.6 h^{-1}, P (H_2) =3.0 MPa, H_2/DMO = 80. [a]TOF (turnover frequency) was obtained by controlling DMO conversion below 30% (see Experimental details in ESI). [b]Others include 1,2-PDO and 1,2-BDO. [b]Au loading=6 wt%. [c]Total metal loading=6 wt%.

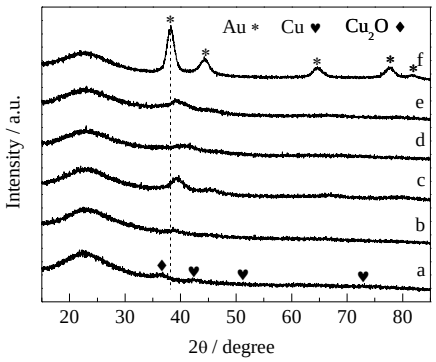

Fig. 1 XRD patterns of $CuAu_x$/SBA-15 with x= (a) 0; (b) 0.05; (c) 0.075; (d) 0.1; (e) 0.2; (f) Au/SBA-15, Au loading=6 wt%.

To investigate the reason behind the improved catalyst performance, *in-situ* XRD, HRTEM, UV-vis, FT-IR and XPS measurements were carried out to get detailed information about the architecture of the catalysts. The *in-situ* XRD patterns of $CuAu_x$/SBA-15 samples indicated that there were remarkable transformations of diffraction lines of Cu and Au species when the reduction temperature was higher than 473 K (Fig. 8s in ESI). Further increasing the reduction temperature up to 673 K brought about no obvious changes in the XRD pattern of $CuAu_{0.1}$/SBA-15. There were four diffraction lines at 2θ=38.2°, 44.3°, 64.5° and 77.6° in the XRD pattern of Au/SBA-15 catalyst, corresponding to Au(111), (200), (220), (311) lattice planes, respectively (Fig. 1).[19] Very weak diffraction peaks could be observed in the XRD pattern of Cu/SBA-15 catalyst, suggesting the formation of maller Cu NPs on the SBA-15 support. The $CuAu_x$/SBA-15 catalysts showed a broad XRD diffraction line at around 2θ=42.9°, assignable to Cu-Au alloy species.[20] With the increase of Au content, this line slightly shifted to higher position and reached a maximum when the atomic ratio of Au to Cu was 0.1, which indicates that the $CuAu_{0.1}$/SBA-15 catalyst has a highest extent of alloying.[21] As for the the UV-Vis diffuse reflection spectroscopy (Fig. 9s in ESI), the Au/SBA-15 presented a single and strong absorption peak at 519 nm, while the Cu/SBA-15 gave a very weak absorption peak at 581 nm. For the $CuAu_x$/SBA-15 samples, there was an absorption band positioned between those of Au/SBA-15 and Cu/SBA-15, which suggested the formation of Au-Cu alloy.[22,23] The higher content of alloying in the $CuAu_x$/SBA-15 catalyst resulted in a larger shift of absorption peak. The indications of the UV-Vis diffuse reflection spectra had a same trend as that of the XRD patterns, showing that there was a highest content of alloying in the $CuAu_{0.1}$/SBA-15 catalyst.

The TEM images revealed that the metal particles were uniformly dispersed on the SBA-15 support (Fig. 2, Fig. 3s and 10s in ESI). With the increase of Au/Cu atomic ratio from 0.05 to 0.2, the average particle size slightly increased from 2.8 to 3.7 nm, all of which were smaller than the gold particle size of 4.9 nm in Au/SBA-15. The HRTEM images showed that the crystal spacing measured is 0.236 nm, which can be equal to the spacing of Au(111) lattice planes 0.2355 nm; the crystal spacing measured 0.210 nm in figure b can be good compliance with the Cu(111) lattice planes 0.2087 nm. However, different from either the Au/SBA-15 or Cu/SBA-15, the HRTEM image of $CuAu_{0.1}$/SBA-15 catalyst in Fig. 2 indicated that the two intervals of 0.227 nm and 0.195 nm between the corresponding two lattice fringes were smaller than the (110) and (220) lattice spacings of gold in the Au/SBA-15 catalyst, but larger than the (111) and (200) lattice spacings of copper in the Cu/SBA-15 catalyst, respectively. The included angle around 52° of the two facets in the $CuAu_{0.1}$/SBA-15 is very close to the theoretical value of 54.7° between the (111) and (220) facets of facial center cubic structure, implying that the exposed crystal planes of the $CuAu_{0.1}$/SBA-15 catalyst were dominated by (111) and (220) facets of Au-Cu alloy. The indications again suggested the formation of Au-Cu alloy in the $CuAu_x$/SBA-15 catalysts.

This journal is © The Royal Society of Chemistry [year]

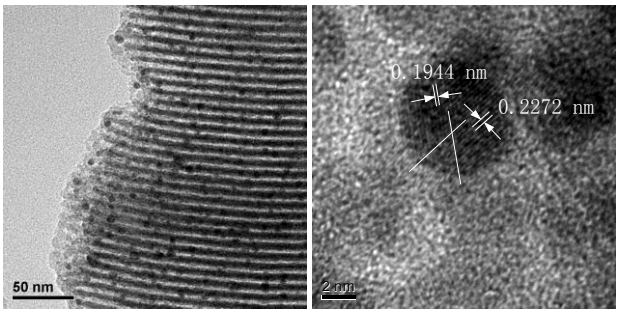

Fig. 2 TEM images of $CuAu_{0.1}$/SBA-15.

Figure 3 displays the IR spectra of CO absorption on as-reduced $CuAu_x$/SBA-15 catalysts. The adsorption of CO on Au/SBA-15 was very weak at room temperature.[17] The intensity of the IR band at 2122 cm^{-1} detected in $CuAu_x$/SBA-15 catalysts varied as the Au/Cu ratio but did not change significantly under the continuous evacuation at room temperature. Assignment of CO absorptions onto Cu^0, Cu^+ and Cu^{2+} surfaces has been well documented in previous work.[7,24-27] The stretching frequency of CO species absorbed onto cupreous surfaces follows the sequence Cu^{2+}–CO > Cu^+–CO > Cu^0–CO, and the CO adsorption onto Cu^0 and Cu^{2+} sites is predominantly weak and reversible at room temperature, while CO linearly bonded with a surface Cu^+ site has higher thermal stability than Cu^{2+}–CO and Cu^0–CO species. According to these assignments, the CO absorption peaks at 2122 cm^{-1} observed on the reduced $CuAu_x$/SBA-15 catalysts should be assigned to Cu^+-CO species. As can be seen from the Fig. 3, with the introduction of gold into the Cu based catalysts, the amount of Cu^+ increased obviously compared with that of the Cu/SBA-15 catalyst, which may result from the formation of Cu-Au alloy. However, with the increase of gold, the amount of Cu^+ decreased gradually, which could be ascribed to the increase of Cu-Au alloy amount on the catalyst surfaces. The presence of Cu^0 and Cu^+ was further evidenced by the Cu XPS and LMM XAES spectra of the catalysts *in situ* treated in 90 kPa H_2 (5%)-Ar (95%) at 623 K for 4 h (Fig. 11s and 12s in ESI). From the deconvolution results (Table 3s), the presence of gold considerably affected the surface Cu^+ and Cu^0 distributions. More Cu^+ species were present at Au/Cu=0.05-0.1. The smaller value of Auger parameter (AP) for Cu^+ than the bulk value was attributed to the strong interactions among Cu^+, SBA-15 and Au. It is reported that when copper species in +2, +1, and 0 valences are highly dispersed states and in intimate contact with the supports, AP value can be 2-3 eV lower than the bulk ones.[28] The results demonstrate that the coexistence of Cu^+ and Cu^0 species on the catalyst surfaces is indispensable for the hydrogenation of DMO to EG.

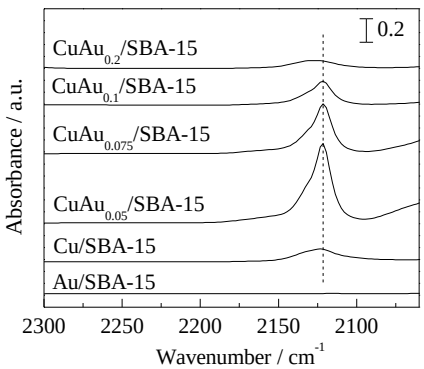

Fig. 3. *In-situ* FT-IR spectra of CO absorption on 623-K reduced $CuAu_x$/SBA-15 catalysts followed by evacuation for 30 min at 298 K.

In summary, we have found that with the introduction of small amount of gold to Cu/SBA-15, the derived $CuAu_{0.1}$/SBA-15 catalyst exhibited remarkably enhancement in the catalytic performance for the hydrogenation of DMO to EG. This catalyst was very active and robust at temperatures ranging 453-493 K and could provide exceptionally EG yield of larger than 1500 mg/g-cat/h. The Cu-Au alloy NPs were formed on the catalyst surface, which are believably beneficial for stabilizing the Cu^0 and Cu^+ distribution and retarding the surface transmigration of Cu species during the hydrogenation process.

This work is supported by the MOST of China (2011CBA00508), the NSFC (21173175), The Research Fund for the Doctoral Program of Higher Education (20110121130002) and the Program for Changjiang Scholars and Innovative Research Team in University (IRT1036).

Notes and references

[a] *Department of Chemistry, College of Chemistry and Chemical Engineering, State Key Laboratory of Physical Chemistry for Solid Surfaces, National Engineering Laboratory for Green Chemical Productions of Alcohols–Ethers–Esters, Xiamen University, Xiamen 361005, China.*

E-mail: yzyuan@xmu.edu.cn; Fax: +86 592 2183047;
Tel: 86 592 2181659
[b] *Catalysis Research Center, Hokkaido University, Kita-ku N21W10, Sapporo, Hokkaido 001-0021, Japan.*
E-mail: askr@cat.hokudai.ac.jp; Tel and Fax: +81-11-706-9113
† Electronic Supplementary Information (ESI) available: Experimental details and characterization data. See DOI: 10.1039/b000000x/

1 J. Yang, L. Gang, L. Wei, W.D Xiao, *J. Mol. Catal. A: Chem.*, 2009, **314**, 63.
2 L.F. Chen, P.J. Guo, M.H. Qiao, S.R. Yan, H.X. Li, W. Shen, H.L. Xu, K.N. Fan, *J. Catal.*, 2008, **257**, 172.
3 *(a)* L.R. Zehner, R.W. Lenton, *US Pat.*, 4112245, 1978; *(b)* F. Poppelsdorf, *EP Pat.*, 0060787, 1982; *(c)* S. Tahara, K. Fujii, K. Nishihira, M. Matsuda and K. Mizutare, *US Pat.*, 4453026, 1984.
4 D.M. Huang, Z.M. Chen, F.X. Chen, P. Lin, H.S. Lan, Y.F. He, *Chin. Ind. Catal.*, 1996, **4**, 24.
5 J.D. Lin, X.Q. Zhao, Y.H. Cui, H.B. Zhang, D.W. Liao, *Chem. Commun.*, 2012, **48**, 1177.
6 A. Yin, X. Guo, W.L. Dai, K.N. Fan, *J. Phys. Chem. C*, 2009, **113**, 11003.
7 Z. He, H.Q. Lin, P. He, Y.Z. Yuan, *J. Catal.*, 2011, **277**, 54.
8 C.L. Bracey, P.R. Ellis, G.J. Hutchings, *Chem. Soc. Rev.*, 2009, **38**, 2231.
9 J.G. Chen, C.A. Menning, M.B. Zellner, *Surf. Sci. Rep.*, 2008, **63**, 201.
10 A. S. K. Hashmi, G J. Hutchings, *Angew. Chem. Int. Ed.*, 2006, **118**, 8064.
11 T.S. Mozer, D.A. Dziuba, C.T.P. Vieira, F.B. Passos, *J. Power Sources*, 2009, **187**, 209.
12 C. Della Pina, E. Falletta, M. Rossi, *J. Catal.*, 2008, **260**, 384.
13 J. Llorca, M. Domínguez, C. Ledesma, R. J. Chimentão, F. Medina, J. Sueiras, I. Angurell, M. Seco, O. Rossell, *J. Catal.*, 2008, **258**, 187.
14 S. Song, R. Liu, Y. Zhang, J. Feng, D. Liu, Y. Xing, F. Zhao, H. Zhang, *Chem. Eur. J.*, 2010, **16**, 6251.
15 A. Yin, C. Wen, W. L. Dai, K.N. Fan, *J. Mater. Chem.*, 2011, **21**, 8997.
16 X. Liu, A. Wang, L. Li, T. Zhang, C.Y. Mou, J.F. Lee, *J. Catal.*, 2011, **278**, 288.
17 J. C. Bauer, D. Mullins, M. Li, Z. Wu, E. A. Payzant, S. H. Overbury, S. Dai, *Phys. Chem. Chem. Phys.*, 2011, **13**, 2571.
18 C.J.G. Van Der Grift, A.F.H. Wielers, B.P.J. Jogh, J. Van Beunum, M. De Boer, M. Versluijs-Helder, J.W. Geus, *J. Catal.*, 1991, **131**, 178.
19 A. Wang, Y.-P. Hsieh, Y.F. Chen, C.Y. Mou, *J. Catal.*, 2006, **237**, 197.
20 S. Pal, G. De, *J. Mater. Chem.*, 2007, **17**, 493.
21 G. De, G. Mattei, P. Mazzoldi, C. Sada, G. Battaglin and A. Quaranta, *Chem. Mater.*, 2000, **12**, 2157.
22 X. Liu, A. Wang, X. Wang, C.Y. Mou, T. Zhang, *Chem. Commun.*, 2008, **27**, 3187.
23 S. Sarangi, A. Hussain, S. Sahu, *Appl. Phys. Lett.*, 2009, **95**, 73.
24 A. Dandekar, M. Vannice, *J. Catal*., 1998, **178**, 621.
25 I. A. Fisher, A. T. Bell, *J. Catal*., 1998, **178**, 153.
26 K. I. Choi, M. A. Vannice, *J. Catal*., 1991, **131**, 22.
27 F. Boccuzzi, A. Chiorino, *J. Phys. Chem. C*, 1996, **100**, 3617.
28 M.A. Kohler, H.E. Curry-Hyde, A.E. Hughes, B.A. Sexton, N. W. Cant, *J. Catal.*, 1987, **108**, 323.

 This journal is © The Royal Society of Chemistry [year]